American Journal of Engineering Research (AJER)
e-ISSN : 2320-0847 p-ISSN : 2320-0936
Volume-03, Issue-1, pp-68-79
www.ajer.org

Research Paper Open Access

Geotechnical Properties of Mixed Marine Sediments on Continental Shelf, Port Sudan, Red Sea, Sudan

Al-Imam, O. A. O.; Elzien, S. M.; Mohammed A. A.; Hussein A.A. Kheiralla, K. M. & Mustafa A.A.

Faculty of Petroleum & Minerals, Al-Neelain University, Khartoum, Sudan

Abstract: **-** Samples from eleven boreholes have been taken from Dama Dama area, which is a part of Sudanese continental shelf. Physical and mechanical properties were investigated with SPT to obtain the bearing capacity and safety factor for engineering properties. The area consists of two facies, which are alluvial mixed with marine deposits and highly to extremely weathered limestone. The computation of effective overburden pressure, N-values were used to predict ultimate and allowable bearing capacity from which the safety factor was calculated and equal 2.5 with final settlement of 2.54mm.

I. INTRODUCTION

The Red Sea region is interesting for geologists, and geotechnical engineers in mining and constructions. The regional geology (Fig. 1) was carried out by Vail (1983, 1989); Babikir (1977); Al Nadi (1984) and Koch (1996). Felton (2002) reported that the modern rock shoreline sedimentary environment is a hostile one and range of high – energy processes characterize these shorelines. The designation of weathering depositional companion model of the karst formation in the Red Sea coast of Sudan had been done by Al-Imam et al., (2013). For solving engineering, geological, hydrogeological and environmental tasks, geo-electrical methods are routinely applied. However, almost the investigations were used the geo-electrical methods in different types of coast formations (Olayinka et al., 1999; Limbrick, K.J. 2003). In contrast, several geotechnical characteristics of soil could be evaluated by using electric resistivity and the correlated with depth and other parameters (Giao et al. 2003).

Very rare geotechnical publications in Sudanese coast on continental shelf even hazard map for engineering purposes, planning and/or development never take any researcher interest. In contrast, intensive investigations have been done on the eastern Red Sea coast. Geotechnical problems as chemical stabilization in Sabkha and formations were studied by Al-Imoudi (1995).

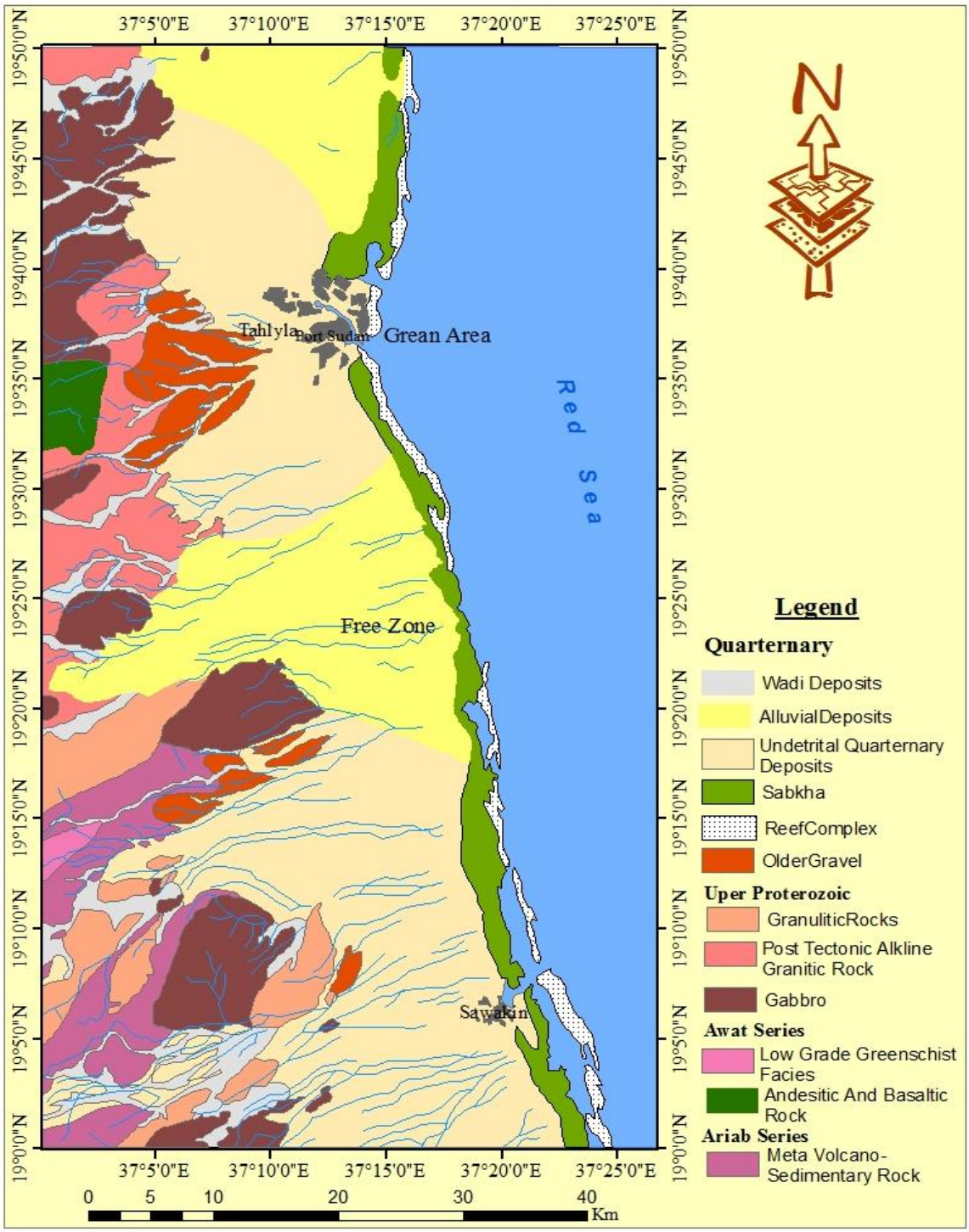

Fig. 1: Regional geological map of the study area

II. LOCATION AND SAMPLING

Dama Dama is located about 7.0km southern Port Sudan (Fig. 2). The site was selected by the Administration of Engineering Projects Department-Sudan Ports Corporation. Eleven boreholes were drilled in mixed alluvial marine deposits on continental shelf (Table 1) using rotary x-y rig on mobile platform. The sampler have thick wall of 89mm thickness, 200mm length and the hammer weight is 63.5kg with length of 810mm. Drop distance is 760mm, tube 51mm and penetration pen 300mm.

Five as sampling boreholes and six for exploration, disturbed and undisturbed samples from different levels were collected and obtained for physical and mechanical tests.

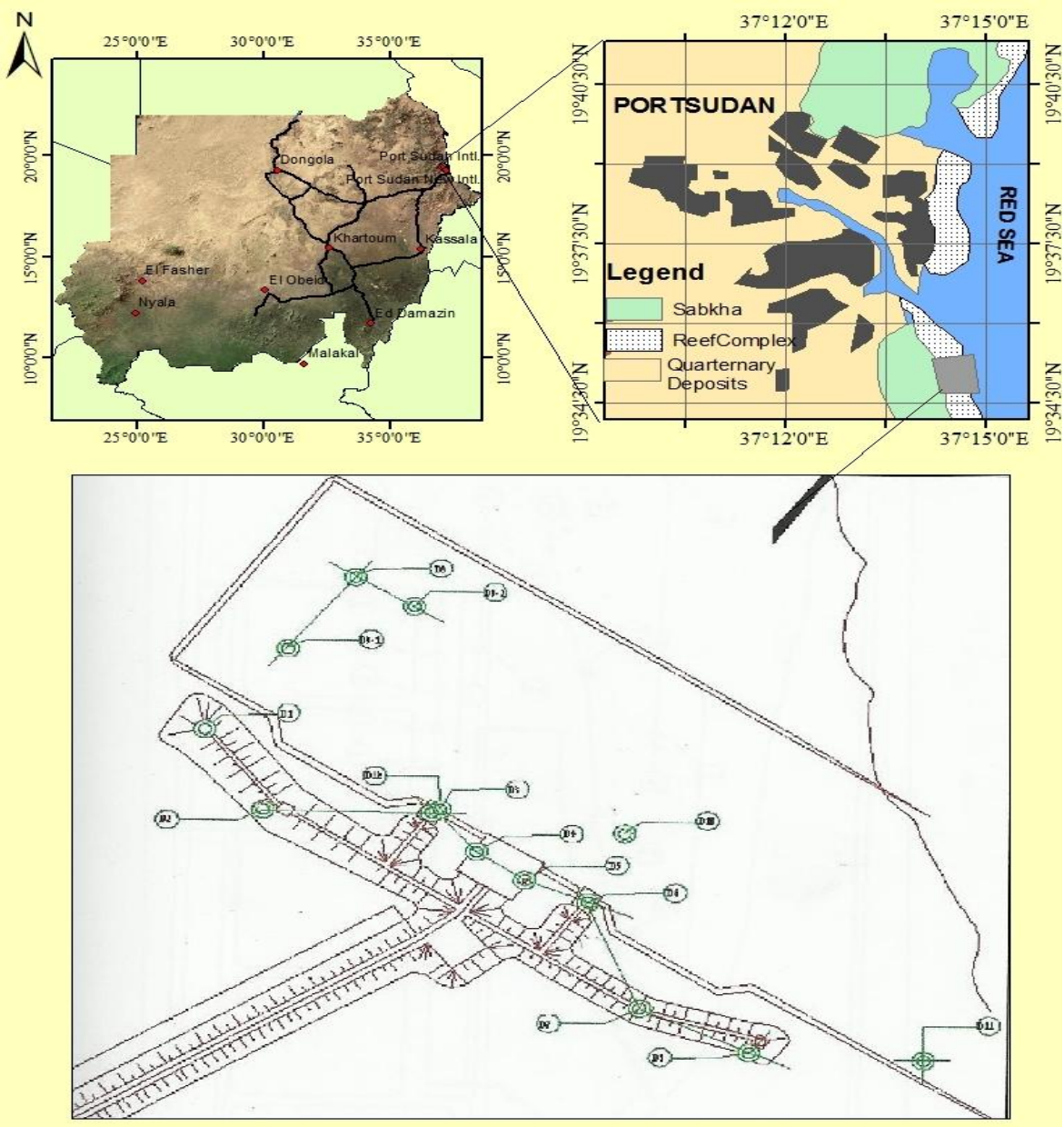

Fig. 2: Location map, shows the boreholes positions

Table 1: Location of boreholes

BH NO.	BH type	Depth (m)	Elevation (m)	Location	
				D (m)	C (m)
1	Explorer	21.70	-18.60	7657.60	11414.70
2	Sampling	22.80	-4.00	7612.00	11439.70
3	Sampling	33.10	-2.70	7610.30	11517.70
4	Explorer	36.00	-0.70	7588.50	11535.90
5	Sampling	34.80	-0.70	7572.10	11557.10
6	Explorer	30.50	-4.60	7560.20	11585.00
7	Sampling	26.00	-0.75	7500.10	11608.60
8	Explorer	24.80	-0.70	7475.80	11657.70
9	Sampling	15.50	-0.80	7741.50	11481.30
10	Explorer	09.25	-7.00	7597.80	11601.40
11	Explorer	06.50	-6.50	7470.60	11735.90

III. METHODOLOGY

Different designations were carefully selected from American Standard Test Methods (ASTM) and BS-59-30 for weathering grade. All data were processed by Rock wares 2004 software in two and three dimensions.

IV. OBJECTIVES

To investigate the marine deposits which consists of mixed alluvial carbonate forming the sea bed by using physical and mechanical properties for stable foundation under prevailing oceanographic conditions.

V. MARINE CONDITIONS

The sea level change is higher from November to May with the maximum in March and lower during June-October with minimum in August (Alzain and Al-Imam, 2002). The regional drop in the sea level (June-September) due to NNW wind which blow over the entire length of the sea (Osman, 1984a). The hydrodynamic condition prevailed and the generated waves towards the shoreline reach heights of order of 30.0cm. The wind velocities occasionally attain gale force producing up to one meter high. The tidal amplitude is 0.3- to 0.4m placing the shore zone in micro tidal environment (Alzain and Al-Imam, 2002).

VI. CORAL REEF LIMESTONE

Before the last regression, the sea level rose by perhaps as much as 20.0m and both positive and negative changes have occurred in the area (Alzain and Al-Imam, 2004). Pliocene and Tertiary deposits exposed to weathering and erosion during marine regression. Braithwaite (1982) suggested that at such times, limestone would have been sculpted into the complex karsts topography. However, the outcrops coral reef limestone in the area almost indicates to synchronous deposition of fossiliferous limestone followed by oolitic and then lime mud. The variability of the shore and shoreline in the area caused by seasonal changes in the climate, oceanographic conditions and drainage system which become active in the interseasonal periods. With the help of the concept of morphologic states the seasonal and interseasonal variability can be assessed qualitatively. Obviously, beach mobility increases with increasing temporal variability of the beach state observed. The alluvial deposits reach the sea floor within the reef area by hydrological process and mixed with reefal sediments.

VII. RESULTS AND DISCUSSION

Values of some representative samples reflect the environment deposition and grain size. The boreholes consist of two types of facies, carbonate and mixed alluvial with marine depositsexcept BH10 and BH11 whichare carbonate as a resultant of variations of environmental conditions. BH1 and BH2 almost are alluvial and the carbonate appears at depth at 22.20m. The Carbonate facies in BHs thickness between 3to8m at depth range between 9.80m to 13.80m. The coral reef of grow stopped at mentioned depths due to intensive accumulation of alluvial deposits by drain system pattern direct to the sea. The thickness of these deposits varies from 6.88m in BH6 to 11.3m in BH3. The marine environment was changed to be suitable for coral reef growing at depth in range of 1.6m to 3.6m up to the bottom surface. Two cycles of mixed deposits appear in BH9 cutting by carbonate facies which have 1.2m thickness. The thickness of the first cycle which overlain the coral reef is 5.6m between depths of 10.6m to 5.0m and the second cycle which covered by coral reef have 2.0m thickness between depths 3.8m to 1,8m. These environmental variations encouraged to weathering of soils and directly affected on its properties, and created a new stratification with the facies according to weathering degree.

1.1. Physical Properties

Table 2 shows some physical properties and consistency of some representative samples. Moisture contents values are indicator for coarse grain soil as well as the apparent specific gravity (Ga) which recorded a relative high values. Wet densityγ_{wet} was determined for each facies and the relative density was empirical value according to Bowles (1984). The distribution of wet density by 2D model (Fig.3a) appeared the weakness zones in the area and it was confirmed by 3D model. Refer to the software scale, where to avoid the values which are less than 1.98 sinkholes like appear due to chemical dissolving for carbonate minerals by sea water (Fig. 3b).

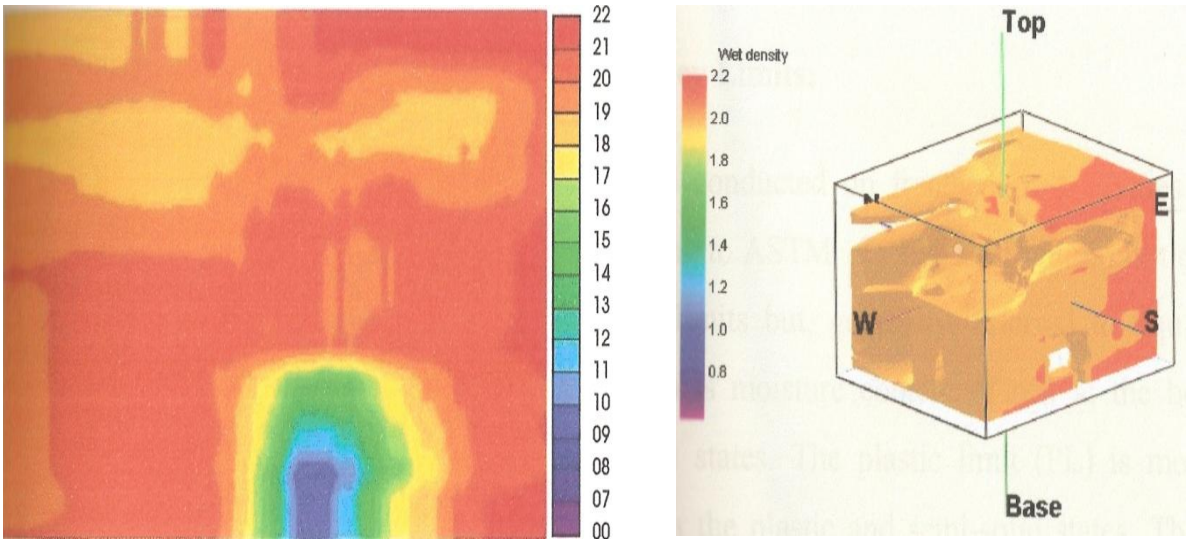

Fig. 3 (a): 2D models of distributions of wet density with depth and (b) 3D bulk model after removing densities less than 1.89, shows sinkhole like in the area

Saturation degree, void ratio values (Table2) were depend on the particle size and show that the alluvial deposits never subjected to high overbarding pressure. However, consistency values liquid limit (LL) and plasticity (PI) were calculated to predict the compression index (C_C) by using the formula:
$C_C = 0.009(L_L - 10)$ for normal consolidation clay. According to the plasticity index (P_I) values show that samples have a values greater than 1.0 means that they are solid clay with $P_I > 17$ which referred to high plastic clay. The relative plasticity index (Rr) was determined for soil condition and moisture content by:
Moisture content- plastic limit/ liquid limit- plastic limit
The application of this formula shows that the values are less than 1.0 in soft state.

Table 2: Physical properties of soil samples

Sample No	Physical properties						Consistency			
	Moisture Content	Specific Gravity	Wet Density	Dry Density	Saturation	Void Ratio	Liquid Limit	Plastic Limit	Plastic Index	Cc
DB2-1	20.9	2.65	1.98	1.46	89.6	0.618				
DB2-4	21.0	2.65	1.87	1.55	77.9	0.715				
DB2-8	20.8	2.65	1.98	1.50	78.5	0.761	22.2	15.6	6.6	0.11
Db2-9							45.3	41.7	3.6	0.32
DB2-10							43.7	30.2	13.5	0.18

1.2. Mechanical Properties

1.2.1. Direct Shear Test

Is adopted from ASTM D3080-72 and samples from BH-2 were obtained to test (Table3). Graph of shear strength versus normal stress (Fig.4) was drowning to predict the cohesion (C) and angle of internal friction (Ø). However, the (C) values are 38.2KPa, 25.5KPa and (Ø) values are 37.4^o and 39.6^o respectively. The results clarify that these types of soils have high internal fraction between particles affected the cohesion intercept (C) and reflected on the internal friction angle. The results confirmed that the friction angle (Ø) of these mixed soils increasing towards the finest particles.

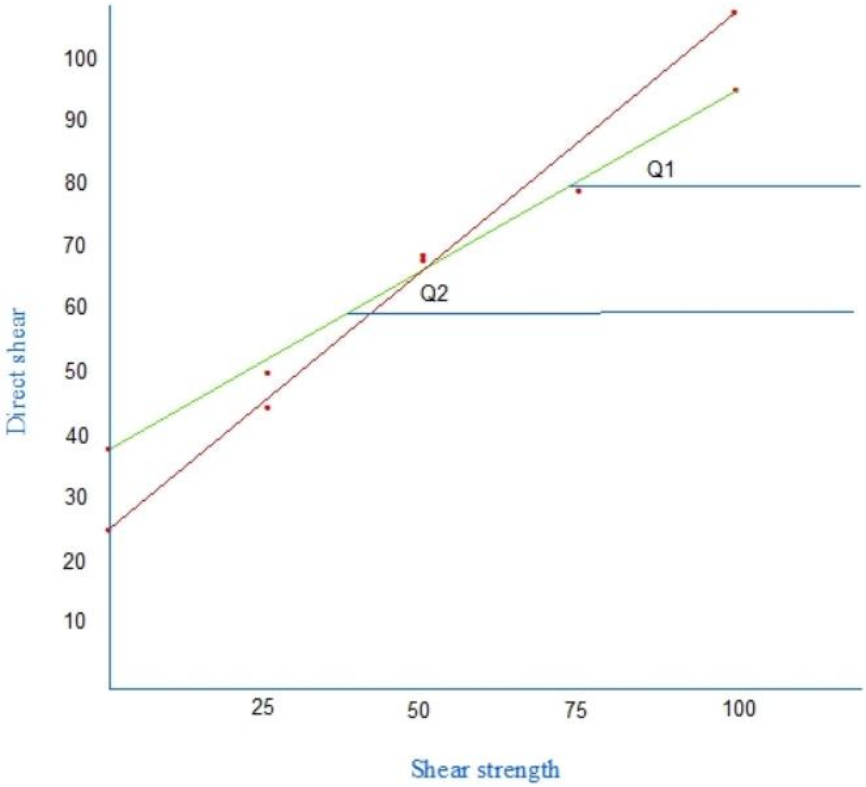

Fig. 4: Shear stress vs direct shear

1.2.2. Compressibility

ASTM D2435-80 has been used for consolidation. The samples were subjected to applied compressive load and allowed to act until equilibrium is reached with corresponding time (24h) and the data graphically presented to evaluate:

- Void ratio versus the load (e-p curve) (Fig. 5a) and (Fig. 5b).
- Time versus deformation (time curve) (Fig. 6a) and (Fig.6b).
- Void ratio versus the log of the pressure after converted to short tour (e-log p).
- Consolidation coefficient versus the log pressure (C_C-log P) curve.

Even more, the e-p curve was used for settlement evaluation and the CC-log P for estimation the time rate of settlement.

The compressibility coefficient (av) obtained from the equation:

$$av = {e_0 - e_1}/{\sigma_1 - \sigma_0}$$

Where: e_o is an initial void ratio, e_1 is a void ratio at 200KPa, σ_1 is 200KPa and σ_o is 100KPa.

Then av equal:

$$av_1 = \frac{0.9908 - 0.978}{200 - 100} = 2 \times 10^{-4} MPa$$

and

$$av_2 = \frac{10 - 0.9753}{200 - 100} = 2.3 \times 10^{-4} MPa$$

The values of (av) can be use to obtain the coefficient of volume change or compressibility (mv) from the formula:

$$mv = {av}/{1 + e_0}$$

Hence:

$$mv_1 = \frac{2 \times 10^{-4}}{1.998} = 1.0 MPa$$

$$mv_2 = \frac{2.3 \times 10^{-4}}{1.998} = 1.15 MPa$$

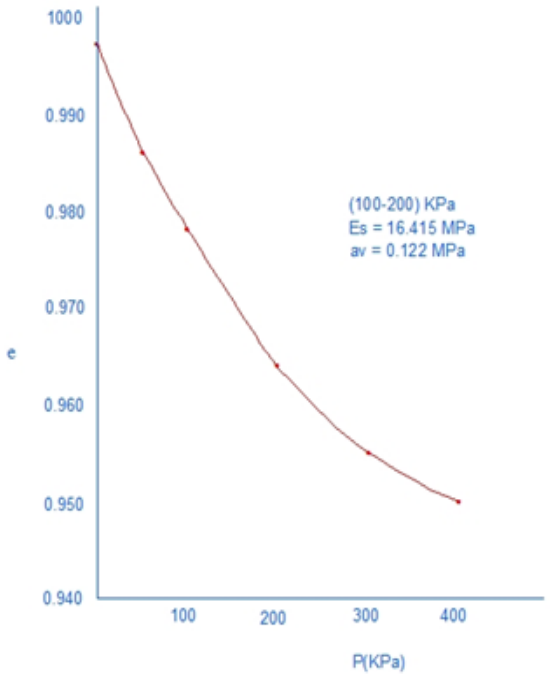

Fig. 5a: e-p curve sample # D2-1

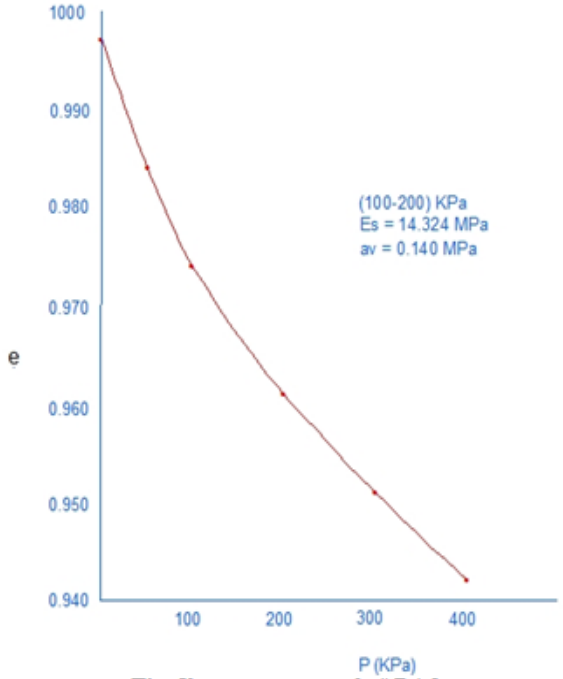

Fig. 5b: e-p curve sample # D4-2

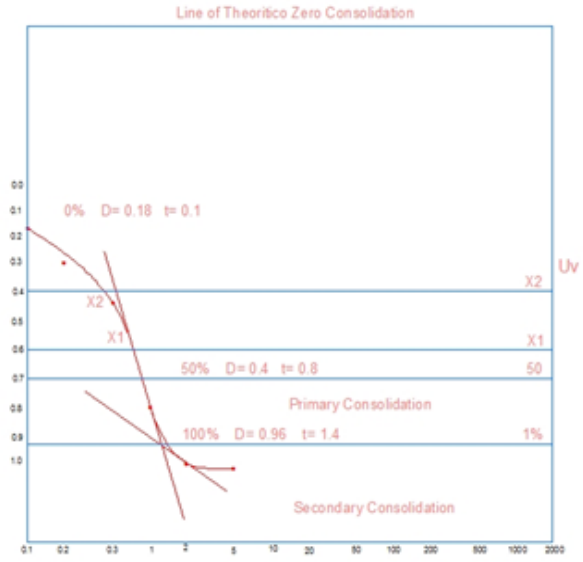

Fig. 6a: Time –consolidation curve, sample # D2-1

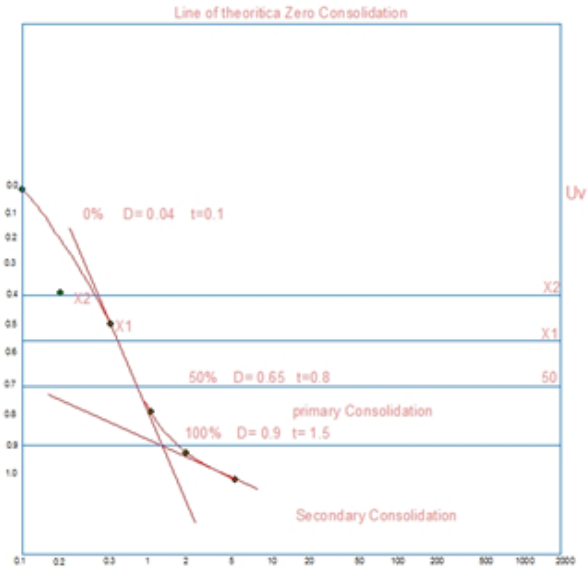

Fig. 6b: Time –consolidation curve, sample # D4-2

Table 3: Mechanical properties of soil samples

Sample No	Direct shear test		Direct shear strength				Compressibility Mode				Compressibility coefficient			
	C KPa	Φ	KPa 25	KPa 50	KPa 75	KPa 100	KPa	KPa	KPa	KPa	KPa	KPa	KPa	KPa
DB2-1	38.2	36.4	50.44	68.39	79.52	95.14	8.14	12.53	16.42	25.73	0.245	0.159	0.122	0.078
DB2-4	25.5	39.6	44.88	69.11		107.7	7.74	10.62	14.32	21.87	0.296	0.188	0.140	00.91

1.2.3. Consolidation Index (CC)

It is a slope of straight line of void ratio versus log load in tannage as shown in Fig (7) which equal 0.05 and 0.02 respectively.

Void ratio and variation in samples height are corresponding to deformation which can compute from height of solids, void ratio, before and after test. By applied load the initial water height, thickness of the sample and void ratio are decrease. The formula is:

$$H_s = \frac{W_s}{A} G_s \gamma_w = H_s = G_s W_s$$

Where,
H_s = Height of initial water.
W_s = weight of dry sample
A = are of specimen
G_s = specific gravity
γ_w = unit weight of water

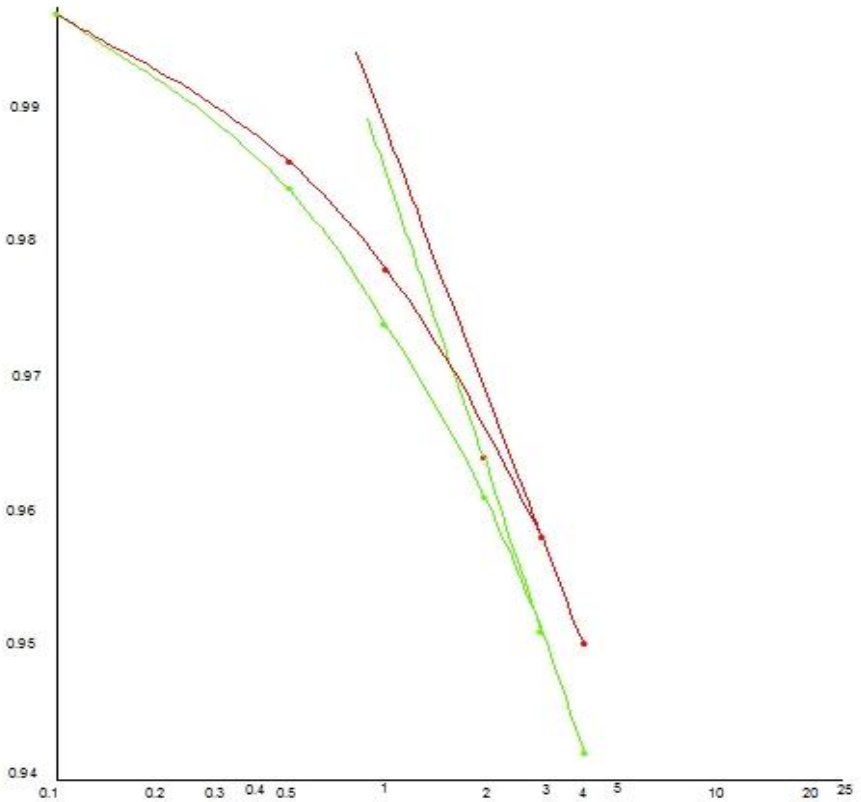

Fig. 7: Void ration vs log load in tonnage to obtained the consolidation index

By calculation the (H_s) equal 20mm before test and (e_o) equal 0.9908 (Fig. 5a) after test. The actual height of the sample after test is:

$$e_0 = H_s - \frac{\Delta H}{H_s}$$

$$0.9908 = 20 - \frac{\Delta H}{20}$$

$$\Delta H = 0.184$$

The results of accumulation ΔH versus time shown in Fig (6a) and Fig (6b) respectively, which can be concentrated into a time – consolidation curve, from which:
For sample (I):
100% deformation (D) = 0.96 at time (t) = 1.4 min.
50% deformation (D) = 0.40 at time (t) = 0.80 min
0.0% deformation (D) = 0.183 at time (t)
For sample (II):
100% deformation (D) = 0.87 at time (t) = 1.5 min
50% deformation (D) = 0.60 at time (t) = 0.70 min
0.0% deformation (D) = 0.0 at time (t)

1.2.4. Consolidation coefficient (Cv)

It is obtained from time-curve by using the formula:

$$C_y = \frac{T_y d^2}{t}$$

Where, T_v was determined from the relation between consolidation degree (U_v) and the time factor from time table which designed by Tarzagiki and Peck (1967).
d^2 = ½ samples thickness (H)
t = time
For sample (I)

	X_2	X_1	D_{50}
U_v	0.50	0.60	0.70
T_v	0.197	0.287	0.403
t	0.40	0.0	0.80
1/2H	10	10	10

By the application of consolidation equation the average value of (C_v) as follow:

$$X_2 = \frac{0.197 \times 10^2}{0.40} = 49.25\ mm^2/min$$

$$X_1 = \frac{0.197 \times 10^2}{0.60} = 47.80\ mm^2/min$$

$$D_{50} = \frac{0.197 \times 10^2}{0.80} = 50.37\ mm^2/min$$

$$C_v(average) = 49.14\ mm^2/min$$

The same procedure was followed to predict the average value of (C_v) of sample (II) which was 69.9mm^2/min.

1.2.5. Settlement

Settlement is stress induced but is statistical time dependent accumulation of particle rolling and slipping which results in permanent soil skeleton change (Bowles, 1984). The sum of immediate settlement (Pi) and consolidated settlement (Pc) is the final settlement (Pf) which can be computed by semi-empirical method based on Standard Penetration Test(SPT) values or from (e-p) curve by using the equation

$$Q_{ud} = \frac{H}{1 + e_1(e_1 - e_2)}$$

Or by using the consolidation index (C_c) by the following equation:

$$H/1 + e_1 \times log_{10} P_0 \sigma_2 / P_0$$

The application of Fig (5a and 5b) using the last equation, the settlement in the area as follow:

Sample	P_i (mm)	P_c (mm)	P_f (mm)
1	0.13	2.41	2.54
2	0.13	0.10	0.23

The variation in (P_c) values refer to the different (C_v) values

1.2.6. Standard Penetration Test (SPT)

The (SPT) was used for its simplicity and availability of variety for correlation with other data. When SPT is performed in soil layers containing shell, coral fragments or any other similar material, the sampler may be plug. This will cause the SPT N-value to be much greater than unplugged sampler and therefore, not representative index of soil layer properties. In this circumstance, a realistic design requires reducing the N-values which do not appear distorted (st. of Florida, 2004). The field N-values were corrected by equation depends on the effective overburden pressure proposed by Bazaraa (1967) as follow:

$$P_0 =\geq 75\ KPa \ldots N = \frac{4N}{3.25 + X_2 P_0}$$

Where:
X_1 = 0.4 for SI units.
X_2 = 0.01 for SI units.
P_0 = effective overburden pressure.
The SPT profile of the area (Fig. 8a) shows medium N-values trend to low except small surface area due to the weathering grade. According to the relation between N-values and densities and when to avoid N-values which less than 20 the weakness of the strata appear in 3D model (Fig. 8b).

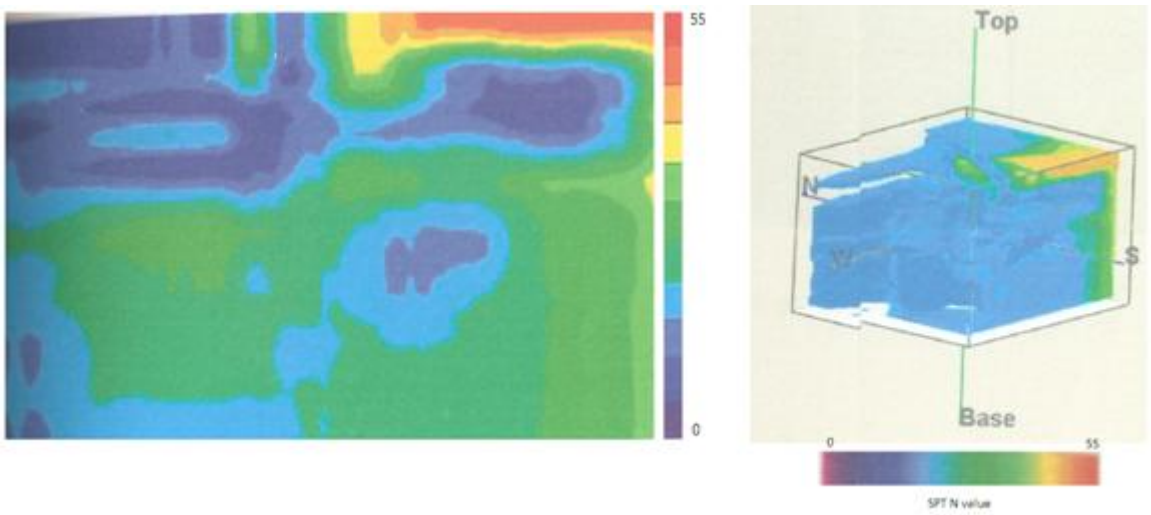

Fig. 8 (a):. 2D models of N value and (b) 3D of N value >20

1.2.7. Bearing Capacity by (SPT)

The general equation of bearing capacity depends on both, angle of internal friction (Ø) and total overburden pressure (TOP). To determine the (Ø) value the standard curve of the relationship between SPT (N-values) and angle of shear resistance (Peak, Hanson and Thorburn, 1967) have been used. The general equation of ultimate bearing capacity is:

$$q_{ult} = q'\{(1 + sin\emptyset)/(1 - sin\emptyset)\}^2$$

The values increasing with depth (Fig. 9a) and when avoid values less than 4000 which equal one third of the total value, the strata became as in Fig. (9b).The (q_{ult}) divided by safety factor to obtain the allowable bearing capacity (q_{all}). However, the safety factor depends on type of foundation, load such as dead load (DL) , live load (LL), wind load (WL) and earth pressure (EP) (Bowles, 1984), and he suggested that the values of safety factors between 1.2 to 5.0. In this study, the safety factor is one third of (q_{ult}) and then divided by (3) because the dominant weathering grade is grade III. Subtract another one third and divided the maximum (q_{ult}) by the result as follows, after application of RW software and the safety factor (F) has been change to 4.5:

(q_{ult}) = 10.000

Divide by 3 = 10.000/3 = 3.33

= 3.33/3 = 1.11

3.33-1.11= 2.22

Hence: 10.000/2.22 = 4.5 = F

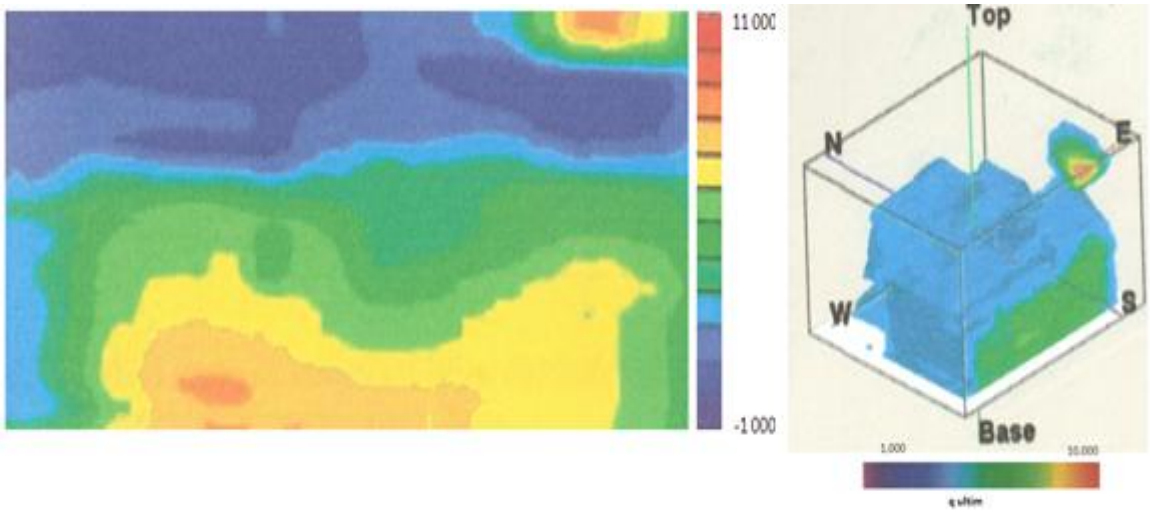

Fig. 9 (a): 2D ultimate bearing capacity and (b) 3D ultimate bearing capacity less than 4000

The (q_{all}) have the same shape with slightly less in value (Fig. 10) comparing with Fig. (9b).This confirmed the results and the relation between density and N-value.

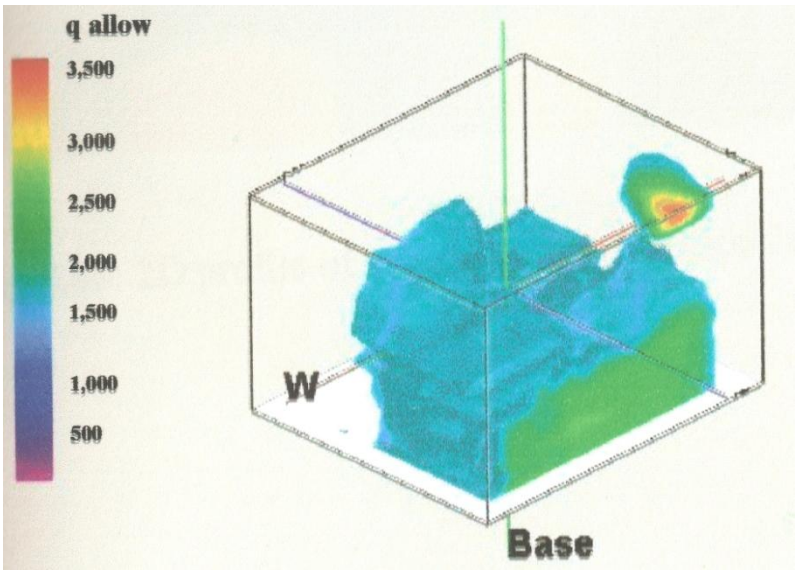

Fig. 10.3D: allowable bearing capacity

VIII. CONCLUSION

The sea water is a geotechnical system having direct efficiency on soil and reef limestones causing weathering and corrosion by chemical reactions. The reef limestones in the region are completely and extremely weathered, having varies bearing capacity. Both specific gravity (G_s) and dry density (γ_{dry}) values in contrast of wet density (γ_{wet}) and saturation values give an indication of mixture of alluvial marine deposits. The intensive cavities are characteristic the region and can be developed to be sink holes. Although, the mechanical parameters values give an encouragement for engineering construction, all foundation in the area and/or which like must be pilling design with taken case in soil geotechnical profile.

REFERENCES

[1] **Al-Amoudi, O.S.B., (1993).** Chemical Stabilization of Sabkha soils at high moisture contents. Eng. Geol., 36:279-291.

[2] **Al-Imam O.A.O; ElsayedZeinelabdein, K.A., and Elsheikh A.E.M. (2013).** Stratigraphy and subsurface weathering grade investigation for foundation suitability of Port-Sudan-Suakin area, Red Sea region, NE Sudan. SJBS, Series (G), U of K, Sudan (in press).

[3] **Al-Zain, S.M.& Al-Imam, O.A.O., (2002).** Carbonate Minerals diagenesis in Towaratit Coastal Plain, south Port-Sudan, Red Sea, Sudan. Nile Basin Research Journal .Alneelain University, Khartoum, Issue No. 4, Vol. II p35 – 58.

[4] **Al-Zain, S.M.& Al-Imam, O.A.O., (2004).**Sea Level Changes and Evolution of Towaratit Coastal Plain south Port-Sudan, Red Sea, Sudan. Nile Basin Research Journal Alneelain University, Khartoum, Issue No. 6, Vol.III, p 32-54.

[5] **Babikir, I.M., (1977).**Aspects of the Ore Geology of Sudan. Ph.D. Thesis. University College of Cardiff. U.K.

[6] **Bazaraa A. R. (1967).** Use of stander Penetration Test of estimating settlements of shallow foundation on sand.PhD. Thesis. Uni. Illinois, Urban, pp. 379.

[7] **Bowles. J. E. (1984).** Foundation analysis and design. 3rd ed McGraw-Hill International, London.

[8] **Braithwaite, C. J. R. (1982).** Geomorphology accretion of reef in the Sudanese Red Sea. Mar. Geol., 46:297-325

[9] **El Nadi, A.H., (1984).**The geology of the Precambrian metavolcanics. Red Sea Hills, NE Sudan. PhD. Thesis. University of Nottingham, England, UK.

[10] **Felton, E.A. (2002).** Sedimentology of rocky shorelines: 1. A review of the problem, with analytical methods, and insights gained from the Hulopoe gravel and the modern rocky shoreline of Lanai, Hawaii. Sedimentary Geology 152, 221–45.

[11] **Giao, P.H., Chung, S.G., Kim, D.Y., Tanaka, H. (2003).** Electrical imaging and laboratory resistivity testing for geotechnical investigation of Pusan clay deposits. Journal of Applied Geophysics 52, 157–175.
[12] **Koch.W.(1996).**Analyseund Visualisie runggeo wissen schaftlicher Datenmit Hil fedigitaler Bildverar beitung und eines Geo-Informations systems: Beitrag zurregionalen Geologie der Red Sea Hills, Sudan: geologischeKarte Port Sudan 1:250 000 und Blatt Jebel Hamot 1:100 000. Berliner GeowissenschaftlicheAbhadlungen, Reiche D Band 12.
[13] **Limbrick, K.J. (2003).** Baseline nitret concentration in groundwater of ckalk in south desert, UK. The Sci. of the total environ. 314-316. 89-98
[14] **Olayinka, A. I.; Abimbola, A. F.; Isibor, R. A.; Rafiu, A. R. (1999).** Ageo-electrical hydrothermal investigation of shallow groundwater occurrence in Ibadan, Southwest Nigeria,. Environ. Geol. Vol. 37:31-39
[15] **Osman, M. M. (1984a).** Evaporation off water in port Sudan. Jour of the Fac. Mar. Sci., KAU. S Arabia. 4:29-37
[16] **Peak, Hanson and Thorburn.(1967).** Foundation design engineering 2ed ed. John Willey, New York. P310.
[17] St. of Florida. (2004). Soils and foundations handbook: Dept. of Transportation, State Materials office, Gainesvlle, Florida, USA.
[18] **Tarzagiki K: Peck, R. B. (1967).** Soil mechanics in engineering practices 2ed ed. John Willy New York. Pp 341-347.
[19] **Vail, J. R. (1983).** Pan- African Crustal Accretion in NE Africa. Jour. Earth Society, 1:285-294
[20] **Vail, J. R. (1989).** Tectonic and evolution of the Proterozoic Basement of NE Africa. In: Elgaby, S. and R. O. Greiling (Eds). The Pan-African belts of NE Africa and adjacent areas. Fried Uieweg and Sohu: 185-226.